

CERN-TH.7244/94  
IUHET-279

## THE ELECTROWEAK PHASE TRANSITION AT $m_H \simeq m_W$

K. Farakos<sup>a1</sup>, K. Kajantie<sup>b</sup>, K. Rummukainen<sup>c</sup> and M. Shaposhnikov<sup>d2</sup>

<sup>a</sup>*National Technical University of Athens, Physics Department,  
Zografou Campus, GR 157 80, Athens, Greece*

<sup>b</sup>*Department of Theoretical Physics, P.O. Box 9, 00014 University of Helsinki,  
Finland*

<sup>c</sup>*Indiana University, Department of Physics, Swain Hall West 117,  
Bloomington IN 47405, USA*

<sup>d</sup>*Theory Division, CERN,  
CH-1211 Geneva 23, Switzerland*

### Abstract

We study the finite temperature electroweak transition with non-perturbative lattice Monte Carlo simulations. We find that it is of first order, at least for Higgs masses up to 80 GeV. The critical temperature of the phase transition is found to be smaller than that determined by a 2-loop renormalization group improved effective potential. The jump of the order parameter at the critical temperature is considerably larger than the perturbative value. By comparing lattice data and perturbation theory, we demonstrate that the latter, for the computation of the vacuum expectation value of the Higgs field  $v(T)$  in the broken phase at given temperature, converges quite well, provided  $v(T)/T > 1$ . An upper bound on the Higgs mass necessary for electroweak baryogenesis in the light of the lattice data is briefly discussed.

CERN-TH.7244/94  
May 1994

---

<sup>1</sup>Partially supported by a CEC Science program (SCI-CT91-0729).

<sup>2</sup>On leave of absence from the Institute for Nuclear Research of the Russian Academy of Sciences, Moscow 117312, Russia.

# 1 Introduction

The high-temperature limit of the 4-dimensional electroweak theory near the phase transition and for sufficiently large Higgs masses can be described by an effective 3-dimensional gauge-Higgs theory (for a discussion of high-temperature phase transitions see [1], for a general consideration of dimensional reduction see [2], for 3d EW theory see [3, 4, 5]). The effective theory is strongly coupled in the symmetric phase [6, 7]; in particular, pure  $SU(2)$  gauge theory in 3d is confining. This fact makes a reliable *entirely perturbative* computation of almost all characteristics of the phase transition impossible. For example, the computation of the critical temperature  $T_c$  requires the comparison of the vacuum energy of the symmetric and broken phases, and the former cannot be estimated on perturbative grounds. The bubble nucleation temperature  $T^*$  in cosmology is related to the structure of the effective action for small scalar fields, which is precisely the place where infrared divergences are most severe. The expectation value of the Higgs field  $v(T^*)$  at the temperature  $T^*$ , necessary for the estimate of the fermion number non-conservation rate [8], cannot be found perturbatively, just because  $T^*$  is non-perturbative. At the same time, the determination of the vacuum expectation value of the Higgs field in the broken phase at a *given* temperature  $T$  by perturbation theory does not require any information on the symmetric phase and may be good enough provided that the ratio  $v(T)/T$  is sufficiently large. Therefore, the study of the nature of the electroweak phase transition requires non-perturbative methods. The most straightforward ones are lattice Monte-Carlo simulations.

First lattice Monte Carlo results on the electroweak phase transition using a 3d effective theory have already been given in [4] (for 4d simulations see [9]). We improve here the analysis of [4] in two ways: by going from the 1-loop to the 2-loop level in the discussion of the 3d effective theory and its effective potential, and by extending considerably the numerical calculations. We find that the EW phase transition is of the first order at  $m_H \simeq m_W$ . The critical temperature we determined is smaller than that following from the perturbative analysis, while the jump of the order parameter is larger. At the same time, 2-loop effective potential gives an adequate description of the order parameter in the *broken* phase for  $v(T)/T > 1$ . These results are in a qualitative agreement with a picture of the electroweak phase transition suggested in [10]. Given the information provided by lattice simulations we comment shortly on the question of the Higgs mass necessary for electroweak baryogenesis [11, 10].

The advantages of considering the effective 3d vacuum gauge-Higgs system in comparison with the full 4d theory at non-zero temperatures have already been discussed in [4] (from the lattice point of view) and in [3] (from the perturbation theory point of view). In the present paper, for reasons of simplicity, the  $U(1)$  factor of the complete electroweak theory is disregarded. The fermionic contributions are omitted as well<sup>3</sup>.

The paper is organized as follows. In Section 2 we briefly summarize the results

---

<sup>3</sup>The most important fermionic contribution is that of the top quark to the effective scalar mass at high temperatures. It does change the absolute value of the critical temperature, decreasing it, but changes only marginally dimensionless ratios such as  $v(T_c)/T_c$ , most important for cosmological applications.

from the perturbative analysis. The lattice action is given in Section 3, as well as a discussion on relating lattice numbers to physical quantities. Numerical results are presented in the Section 4. Section 5 is discussion.

## 2 Continuum Lagrangian

The continuum Lagrangian of the effective 3d theory under consideration is

$$S_{\text{eff}} = \int d^3x \left\{ \frac{1}{4} F_{ij}^a F_{ij}^a + \frac{1}{2} (D_i A_0)^a (D_i A_0)^a + (D_i \phi)^\dagger (D_i \phi) + \frac{1}{2} m_D^2 A_0^a A_0^a + \frac{1}{4} \lambda_A (A_0^a A_0^a)^2 + m_3^2 \phi^\dagger \phi + \lambda_3 (\phi^\dagger \phi)^2 + h_3 A_0^a A_0^a \phi^\dagger \phi \right\}. \quad (1)$$

It contains gauge fields together with the Higgs doublet and a scalar triplet (the former time component of the gauge field). Here all bosonic fields have the canonical dimension  $[\text{GeV}]^{\frac{1}{2}}$  and 3d gauge and scalar couplings  $g_3^2$ ,  $\lambda_3$ ,  $\lambda_A$  and  $h_3$  have dimension  $[\text{GeV}]$ . The relation between 4d and 3d coupling constants and masses on the 1- and 2-loop levels has been discussed in [3]. For all numerical and analytical work we use the following simplified relations:

$$g = \frac{2}{3}, \quad g_3^2 = g^2 T, \quad \lambda_3 = \frac{1}{8} g_3^2 \frac{m_H^2}{m_W^2}, \quad h_3 = \frac{1}{4} g_3^2, \quad \lambda_A = 0. \quad (2)$$

Due to the super-renormalizability of the 3d theory (only a finite number of diagrams are divergent) these relations are scale-independent<sup>4</sup>. The Debye screening mass and the effective Higgs mass are [3]

$$m_D^2 = \frac{5}{6} g^2 T^2, \quad (3)$$

$$m_3^2(\mu_3) = \left[ \frac{3}{16} g_3^2 T + \frac{1}{2} \lambda_3 T + \frac{g_3^2}{(4\pi)^2} \left( \frac{149}{96} g_3^2 + \frac{3}{4} \lambda_3 \right) \right] - \frac{1}{2} m_H^2 + \frac{1}{16\pi^2} \left[ f_{2m} \left( \log \frac{3T}{\mu_3} + c \right) \right]. \quad (4)$$

The numerical constant  $c = -0.348725$ , the parameter  $\mu_3$  is the scale of the  $\overline{\text{MS}}$  scheme. The Debye screening mass  $m_D$  is a 3d renormalization group invariant, but the effective Higgs mass runs with the normalization point due to logarithmic divergences on the 2-loop level. The 2-loop coefficient  $f_{2m}$  is given by

$$f_{2m} = \frac{81}{16} g_3^4 + 9\lambda_3 g_3^2 - 12\lambda_3^2. \quad (5)$$

The 2-loop renormalization group improved effective potential for this theory has been computed in [3]. (The computation of the high-temperature limit of the 2-loop effective potential in 4d has been performed in [12]). We do not write the expression here for lack of space and just mention that, for  $m_H = 80$  GeV and  $m_W = 80.6$  GeV, the critical temperature and the expectation value of  $\phi$  at  $T_c$  in the broken phase computed from it are  $T_c = 173.3$  GeV and  $v(T_c) = 81$  GeV ( $v(T_c)/T_c = 0.47$ ).

---

<sup>4</sup>The actual value of the coupling  $\lambda_A$  is rather small,  $17g^4 T / (48\pi^2)$ . We included this coupling in the lattice simulations just to make sure that the lattice action is bounded from below for constant fields, and checked that the results are independent of  $\lambda_A$  provided that it is small enough.

### 3 The lattice action

Going over to a  $2 \times 2$  matrix representation  $\Phi = (\phi_0 + i\sigma_i\phi_i)/\sqrt{2}$  of the doublet scalar field, discretising and scaling the continuum fields by

$$igaA_0 \rightarrow A_0, \quad \Phi \rightarrow \sqrt{\frac{T\beta_H}{a}}\Phi, \quad (6)$$

the lattice action corresponding to the continuum action in eq. (1) becomes, in standard notation,

$$\begin{aligned} S = & \beta_G \sum_x \sum_{i<j} \left(1 - \frac{1}{2}\text{Tr } P_{ij}\right) + \\ & + \frac{1}{2}\beta_G \sum_x \sum_i [\text{Tr } A_0(\mathbf{x})U_i^{-1}(\mathbf{x})A_0(\mathbf{x}+i)U_i(\mathbf{x}) - \text{Tr } A_0^2(\mathbf{x})] + \\ & + \sum_x \left\{ 10\Sigma - \frac{5}{3}\frac{4}{g^2\beta_G} \right\} \frac{1}{2}\text{Tr } A_0^2(\mathbf{x}) + \\ & + \sum_x \frac{g^2\beta_G}{3\pi^2} \left(\frac{17}{16}\right) \left(\frac{1}{2}\text{Tr } A_0^2(\mathbf{x})\right)^2 + \\ & + \beta_H \sum_x \sum_i \left[ \frac{1}{2}\text{Tr } \Phi^\dagger(\mathbf{x})\Phi(\mathbf{x}) - \frac{1}{2}\text{Tr } \Phi^\dagger(\mathbf{x})U_i(\mathbf{x})\Phi(\mathbf{x}+i) \right] + \\ & + \sum_x \left[ (1 - 2\beta_R - 3\beta_H) \frac{1}{2}\text{Tr } \Phi^\dagger(\mathbf{x})\Phi(\mathbf{x}) + \beta_R \left(\frac{1}{2}\text{Tr } \Phi^\dagger(\mathbf{x})\Phi(\mathbf{x})\right)^2 \right] + \\ & - \frac{1}{2}\beta_H \sum_x \left[ \frac{1}{2}\text{Tr } A_0^2(\mathbf{x}) \frac{1}{2}\text{Tr } \Phi^\dagger(\mathbf{x})\Phi(\mathbf{x}) \right]. \end{aligned} \quad (7)$$

where  $\Sigma = 0.252731$ .

All the three lattice coupling constants are given in terms of  $g, T$  and  $m_H$  by the following equations, which directly follow from the discretisation procedure:

$$\beta_G = \frac{4}{g^2} \frac{1}{Ta}, \quad (8)$$

$$\beta_R = \frac{1}{4}\lambda Ta\beta_H^2 = \frac{m_H^2}{8m_W^2} \frac{\beta_H^2}{\beta_G}. \quad (9)$$

The tree relation between the mass parameter  $m_3$  and the lattice variables is given by

$$m_3^2 = \frac{2(1 - 2\beta_R - 3\beta_H)}{\beta_H a^2}. \quad (10)$$

The 1-loop counterterm ( $\sim 1/a$ ) removing divergences from the Higgs mass has been determined in [4], and the 2-loop counterterm  $\sim \log(a)$  has been estimated in [3]. For present lattices the linear counterterm, included in [4], is clearly the dominant one, but the accuracy of the calculations is already such that the effects of the logarithmic

counterterm are clearly seen. No other counterterms exist since the 3d theory is super-renormalizable.

The knowledge of these counterterms allows one to relate lattice parameters to the temperature:

$$\begin{aligned} \frac{m_H^2}{4T^2} = & \left(\frac{g^2\beta_G}{4}\right)^2 \left[ 3 - \frac{1}{\beta_H} + \frac{m_H^2}{4m_W^2} \frac{\beta_H}{\beta_G} - \frac{9}{2\beta_G} \left(1 + \frac{m_H^2}{3m_W^2}\right) \Sigma - \right. \\ & - \frac{1}{2} \left( \frac{9}{4\pi\beta_G} \right)^2 \left( 1 + \frac{2m_H^2}{9m_W^2} - \frac{m_H^4}{27m_W^4} \right) \left( \log \frac{g^2\beta_G}{2} + \eta \right) \left. \right] \\ & + \frac{g^2}{2} \left[ \frac{3}{16} + \frac{m_H^2}{16m_W^2} + \frac{g^2}{16\pi^2} \left( \frac{149}{96} + \frac{3m_H^2}{32m_W^2} \right) \right]. \end{aligned} \quad (11)$$

Because of the super-renormalizability of the 3d theory, this relation is exact in the continuum limit. On the 1-loop level the analogous relation has been derived in [4]. The determination of the ( $m_H/m_W$  dependent) constant  $\eta$  requires a computation of the 2-loop effective potential of the theory by the lattice perturbation theory and a comparison of the result with the corresponding expression in the  $\overline{\text{MS}}$  scheme. Due to the complexity of this computation, it is not attempted here. Instead, we determine the constant  $\eta$  by Monte-Carlo methods.

## 4 Lattice results

The continuum limit corresponds to  $\beta_G \rightarrow \infty$ ,  $N/\beta_G \rightarrow \infty$ , with  $N$  being the lattice size. Too large a  $\beta_G$  makes the system hard to simulate and we have used  $\beta_G = 12, 20, 32$ . Our computer resources have permitted us to perform runs on lattices of sizes  $8^3 \dots 32^3$ . The confining property of the symmetric phase must not be lost, and this requires

$$\beta_G < 1.468N, \quad (12)$$

at least for pure 3d SU(2) gauge theory [13]. The use of different values of  $\beta_G$  and  $N$  is important to study the scaling and consistency of the results.

Simulations have also been carried out for the Higgs masses  $m_H = 35, 60, 70, 80$  and  $90$  GeV. We will discuss here in some detail only those simulations with  $80$  GeV Higgs (other Higgs masses are discussed in [14]).

The first question is the very existence of the first-order phase transition. To answer it, we searched for a two-peak signal in the distributions of the different order parameters (such as length of the Higgs field  $R^2$ , the average of the link operator  $L = \text{Tr } V^\dagger(x)U_i(x)V(x+i)$ , where  $\Phi = RV$ , etc.) A typical picture at  $\beta_H = 0.347710$ ,  $\beta_G = 12$  and  $V = 24^3$  is shown in Fig. 1. The two-peak structure is clearly seen. At the same time, due to the fact that the lattice volume is finite, the width of any of the peaks is comparable with the distance between them. For comparison, we present in Fig. 2 the distribution of  $R^2$  for a Higgs mass  $m_H = 35$  GeV, where finite-size effects are less important.

The determination of the critical value of  $\beta_H^c$  in the continuum limit requires the analysis of finite-size effects. In principle, a number of different methods can be used

for its determination:

- (i) Equal-area signal. The value of  $\beta_H^c$  is determined as the value of  $\beta_H$  for which the areas [15] under the two peaks in the distribution of some order parameter (actually, it does not matter which order parameter is chosen) are equal.
- (ii) One looks for a maximum of the heat capacity (action susceptibility), considered as a function of  $\beta_H$  [15, 16].
- (iii) The same as in (ii), but for  $L$ -susceptibility [16, 17].

All three methods must give the same results in the continuum limit. For finite lattices and for finite  $\beta_G$  the results are different, and the continuum limit should be found by extrapolation.

The first method works well for small Higgs masses, such as 35 GeV, since the two peaks are well separated, but it cannot be applied with good accuracy to the study of the phase transition with heavy enough Higgses, at least for the lattice sizes we used. So, we used (ii) and (iii) to determine  $\beta_H^c$ . To find the maximum values, we used the Ferrenberg-Swendsen multihistogram method [17], which yields Monte Carlo observables as continuous functions in  $\beta_H$  around the actual  $\beta_H$ -values used in the simulations. The error analysis was performed with the jackknife method.

The results of the determination of the critical  $\beta_H^c$  are shown in Fig. 3 ( $\beta_G = 12$ ) and Fig. 4 ( $\beta_G = 20$ ) as a function of  $1/N^3$ , with  $N = 8, 12, 16, 20, 24$  and  $32$  (without the point  $N = 20$  for  $\beta_G = 20$ ). One can see that both methods give consistent results for sufficiently large volumes of the lattice.

The extrapolation of these results to infinite volume requires some care. For  $\beta_G = 12$  eq. (12) gives  $N > 8$ . The  $\beta_G = 12$  data for  $N \geq 12$  can be fitted very well by a linear function  $\beta_H^c(V) = \beta_H^c(\infty) + c/V$ , giving  $\beta_H^c(\infty) = 0.347703(10)$ . The power low fit  $\beta_H^c(V) = \beta_H^c(\infty) + cV^n$  for all lattice volumes gives a consistent result:  $\beta_H^c(\infty) = 0.347698(12)$  with the power  $n = 0.9 \pm 0.1$ .

For  $\beta_G = 20$  finite-size effects are more important. From eq. (12) one gets for  $\beta_G = 20$   $N > 14$ , so that one to two points at the right of Fig. 4 cannot be trusted. Then, the linear fit with the use of the four largest volumes gives  $\beta_H^c(\infty) = 0.341721(9)$ ; with the three largest volumes,  $\beta_H^c(\infty) = 0.341710(11)$ ; with the three largest volumes,  $\beta_H^c(\infty) = 0.341668(21)$ .

Our final aim is the determination of the critical temperature. To fix it, we must know the parameter  $\eta$  appearing in eq. (11). Since there are no analytic computations of this parameter with the help of lattice perturbation theory (even if they are possible), we determine it by comparison of the results of lattice simulations with perturbation theory deep in the broken phase, where it should work well. We choose the order parameter  $R^2$  for this purpose. In order to relate it to continuum physics one has to subtract from it linear ( $\sim 1/a$ ) and logarithmic ( $\sim \log(a)$ ) divergent terms. It can be shown that  $\langle R^2 \rangle$  is related to the continuum effective potential through

$$\beta_H \langle R^2 \rangle = \left[ 4\Sigma + \frac{3}{2\pi^2\beta_G} \left( \log \frac{3g_3^2\beta_G}{2\mu} + \bar{\eta} \right) \right] + \frac{8}{g_3^2\beta_G} \frac{dV_{eff}(v(T))}{dm_3^2}, \quad (13)$$

where the expression in square brackets contains terms that are divergent in the continuum limit,  $\mu$  is an arbitrary normalization point (the total expression is  $\mu$ -independent

due to the  $\mu$  dependence of the effective potential  $V_{eff}$ ),  $\bar{\eta}$  is unknown constant. The derivative of the effective potential is taken at  $\phi$  in the minimum of the broken phase. In the leading approximation,  $\frac{dV_{eff}}{dm_3^2}|_{v(T)} = \frac{1}{2}v(T)^2$ . The two-loop counter-term contribution to expression (13) is numerically suppressed, so that uncertainties in the determination of  $\eta$  coming from an absence of information about  $\bar{\eta}$  are small provided  $\bar{\eta}$  is not too large (say,  $\bar{\eta} < 2$ ).

The evolution of  $R^2$  distributions in the broken phase with  $\beta_H$  is shown in Fig. 5. In Fig. 6 we show  $\langle R^2 \rangle$  as a function of  $\beta_H$  both as given by lattice data and by 2-loop perturbative computation with parameter  $\eta = 0.54$  ( $\beta_G = 12$ ) and  $\eta = 0.12$  ( $\beta_G = 20$ ). The  $\beta_G = 12$  lattice data corresponds to the variation of  $v(T)/T$  from 1.3 to 2, and  $\beta_G = 20$  data to  $v(T)/T = 1.7\text{--}3.9$ . One can see that the use of 2-loop effective potential for the determination of the vacuum expectation value for the Higgs field in the *broken phase at given temperature* works quite well (numerically  $\frac{\delta v(T)}{v(T)} < 1\text{--}2\%$ ). This means that the dimensionless expansion parameter  $\sim g^2 T/m_W(T)$  is sufficiently small at these temperatures. In other words, non-perturbative effects and higher order terms can be essential numerically only for  $v(T)/T < 1$ .

At the same time, the systematic difference between the lattice data and 2-loop continuum predictions is clearly visible (it is, though, very small, less than 1% in  $\langle R^2 \rangle$ ). In Fig. 7 we show the plot of  $R_{latt}^2 - R_{theor}^2$  as a function of  $\beta_H$  and with the same  $\eta$  choices as in Fig. 6 (the best fits). We suspect that the main source of the difference comes from finite size and finite spacing effects, which are difficult to compute analytically. As a rough estimate of parameter  $\eta$  we take  $\eta = 0.3 \pm 0.5$ , the central value being the average of  $\beta_G = 12$  and  $\beta_G = 20$  best fit values, while the error estimate is the difference between them.

With the value of  $\eta$  determined, the observed values of  $\beta_H^c$  can be converted to results for the critical temperature of the electroweak phase transition using eq. (11). From the  $\beta_G = 12$  data we get  $T_c = 162.1 \pm 2.6$  GeV and from the  $\beta_G = 20$  data quite consistent values  $160.3 \pm 2.6$ ,  $160.9 \pm 2.8$  and  $163.4 \pm 3.0$  GeV, depending on the extrapolation to infinite volume (using four, three, two largest volumes, respectively). One observes that the  $T_c$  determined by lattice methods is clearly smaller than the value  $T_c = 173.3$  GeV determined by perturbative methods.

Since we do not have a clear peak separation at the critical temperature (implying that the system contains, at this temperature, a large fraction of interface configurations interpolating between the broken and symmetric phases) we cannot unambiguously extract from the lattice data at  $T_c$  the quantity  $\langle R^2 \rangle$  relevant for the broken phase only. However, if we take the position of the peak to the right of Fig. 1 as an estimate of  $\langle R^2 \rangle$  in the broken phase, then we see from eq. (13) that  $v(T_c)/T_c = 0.73 \pm 0.04$  (the error estimate is based on the width of the peak). This value may be compared with the results computed in optimized 2-loop perturbation theory:  $v(T_c)/T_c = 0.47$  and  $v(T)/T = 0.81$  for, say,  $T = 163.6$  GeV (which is taken as a "true" critical temperature). We conclude that the true jump of the order parameter (0.73) is clearly larger than that (0.47) coming from perturbation theory. At the same time, the perturbative prediction of  $v(T)$  at  $T = 163.6$  GeV is rather close to the true value (compare 0.73 and 0.81). The difference may be due to the fact that the unambiguous extraction

of  $v(T)/T$  from the distribution of  $R^2$  is not possible and that finite size effects are not small. Another possibility is that at  $v(T)/T \sim 0.7$  deviations (perturbative or non-perturbative) from 2-loop potential predictions are as large as 10%.

## 5 Discussion

The lattice results indicate that the phase transition is more strongly first order than could be expected from perturbation theory. At the same time, a good convergence of the perturbation theory in the broken phase allows us to relate these deviations with the properties of the symmetric phase. At present we cannot extract from available lattice data the parameters relevant for cosmological applications. In particular, the region of metastability of the symmetric phase, together with the bubble nucleation temperature  $T^*$  cannot be determined. The direct lattice determination of  $T^*$  is hardly possible at all, so that some indirect methods are necessary. One of them is related to the measurement of the interface tension at the critical temperature, which allows one to compute the bubble nucleation rate at least in the vicinity of the critical temperature. Another obvious option is to study details of the phase transition for the heavy Higgs boson, since we are approaching the non-perturbative region from the side of the broken phase, increasing  $m_H$ . We plan to return to these questions in future work.

As has been discussed in [10], non-perturbative effects are likely to decrease the value of the potential in the vicinity of the origin. It seems that our lattice results are in a perfect qualitative agreement with this picture. Indeed, consider the plot of the 1-loop and 2-loop renormalization group improved effective potentials at the "true" critical temperature  $T_c^{true} \simeq 163.6$  shown in Fig. 8 (note that the deviation of the 1-loop result from the 2-loop one is negligibly small thanks to the optimization procedure, [3]). Clearly, these potentials are completely wrong at small fields  $\phi$ , since we know that *we are* at the critical temperature. Therefore, the effective potential must have a contribution making the broken and symmetric phases degenerate. According to Fig. 8 this contribution at  $\phi = 0$  equals

$$V_{\text{pert}}(v(T_c)) - V_{\text{pert}}(0) \approx 0.03g_3^6 \approx 60(\alpha_W T)^3. \quad (14)$$

A possible non-perturbative contribution is shown in this picture by a dashed line (in notations of ref. [10], we have taken  $A_F = 0.36$  in the non-perturbative part of the potential). If the specific model for the description of non-perturbative effects considered in [10] is correct, then with this value of the non-perturbative energy shift electroweak baryogenesis may be possible up to a Higgs mass of about 100 GeV. The exact determination of this bound, however, requires a much better understanding of the symmetric phase of the electroweak theory at high temperatures.

## References

- [1] D. A. Kirzhnitz, JETP Lett. 15 (1972) 529;  
D. A. Kirzhnitz and A. D. Linde, Phys. Lett. 72B (1972) 471;

- D.A. Kirzhnitz and A.D. Linde, Ann. Phys. 101 (1976) 195;  
A.D. Linde, Nucl. Phys. B216 (1983) 421, Rep. Prog. Phys. 47 (1984) 925.
- [2] T. Appelquist and R. Pisarski, Phys. Rev. D23 (1981) 2305;  
S. Nadkarni, Phys. Rev. D27 (1983) 917;  
N. P. Landsman, Nucl. Phys. B322 (1989) 498;  
P. Lacock, D. E. Miller and T. Reisz, Nucl. Phys. B369 (1992) 501;  
L. Kärkkäinen, P. Lacock, B. Petersson and T. Reisz, Nucl. Phys. B395 (1993) 733.
  - [3] K. Farakos, K. Kajantie, K. Rummukainen and M. Shaposhnikov, preprint CERN-TH.6973/94, hep-ph 9404201.
  - [4] K. Kajantie, K. Rummukainen and M. Shaposhnikov, Nucl. Phys. B407 (1993) 356.
  - [5] A. Jakovác, K. Kajantie and A. Patkós, Helsinki preprint HU-TFT-94-01, hep-ph-9312355.
  - [6] A.D. Linde, Phys. Lett. 96B (1980) 289.
  - [7] D. Gross, R. Pisarski and L. Yaffe, Rev. Mod. Phys. 53 (1981) 43.
  - [8] V.A. Kuzmin, V.A. Rubakov, and M.E. Shaposhnikov, Phys. Lett. 155B (1985) 36.
  - [9] B. Bunk, E.-M. Ilgenfritz, J. Kripfganz and A. Schiller, Phys. Lett. B284 (1992) 371; Nucl. Phys. B403 (1993) 453.
  - [10] M. Shaposhnikov, Phys. Lett. B316 (1993) 112.
  - [11] M.E. Shaposhnikov. Nucl. Phys. B287 (1987) 757.
  - [12] J.E. Bagnasco and M. Dine, Phys. Lett. B303 (1993) 308;  
P. Arnold and O. Espinosa, Phys. Rev. D47 (1993) 3546;  
Z. Fodor and A. Hebecker, Preprint DESY 94-025 (1994).
  - [13] M. Teper, Phys. Lett. B313 (1993) 417; B311 (1993) 223; B289 (1992) 115.
  - [14] K. Farakos, K. Kajantie, K. Rummukainen and M. Shaposhnikov, “3D physics and the electroweak phase transition: lattice Monte Carlo analysis”, preprint CERN-TH.7220/94, in preparation.
  - [15] H.J. Herrmann, W. Janke and F. Karsch (eds.), Proc. Workshop on Dynamics of First Order Phase Transitions, Julich , June 1992 (World Scientific, Singapore, 1992).
  - [16] C. Borgs, R. Kotecký and S. Miracle-Sole, J. Stat. Phys. 62 (1991) 529.
  - [17] A. M. Ferrenberg and R. H. Swendsen, Phys. Rev. Lett. 61 (1988) 2635.

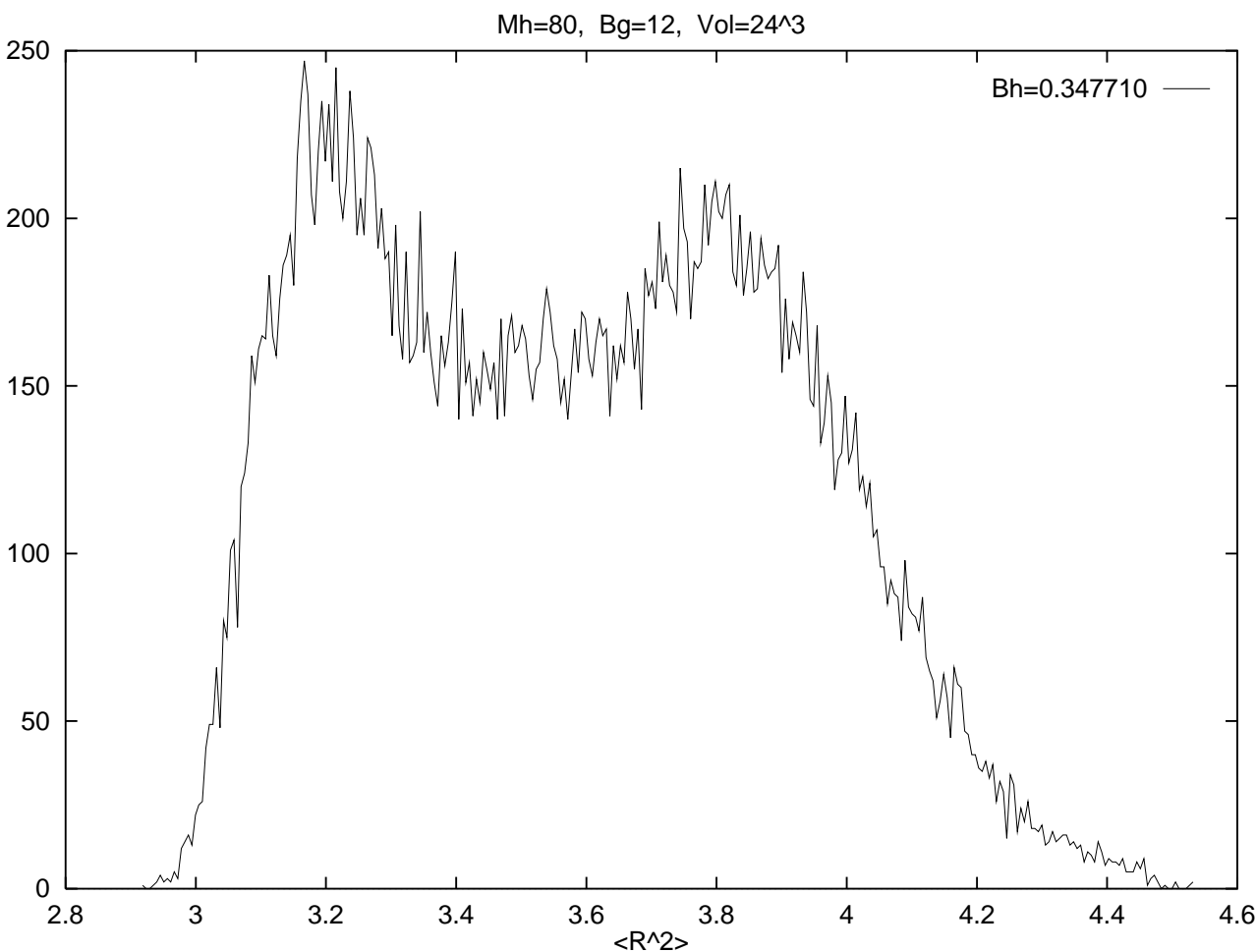


Figure 1: Distribution of the order parameter  $R^2 = \frac{1}{2} \text{Tr} \Phi^\dagger \Phi$  at the critical temperature.

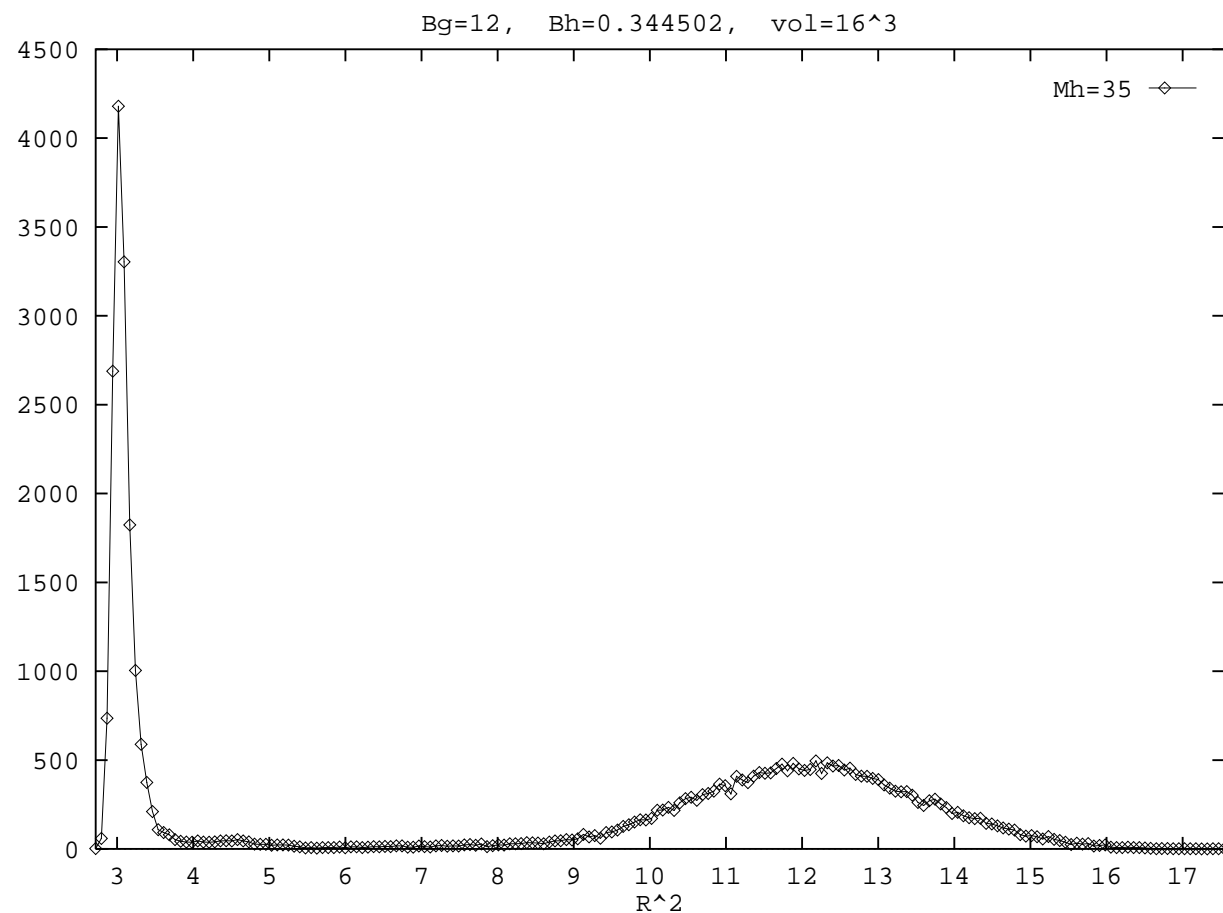


Figure 2: Distribution of the order parameter  $R^2$  at the critical temperature, with  $m_H = 35$  GeV.

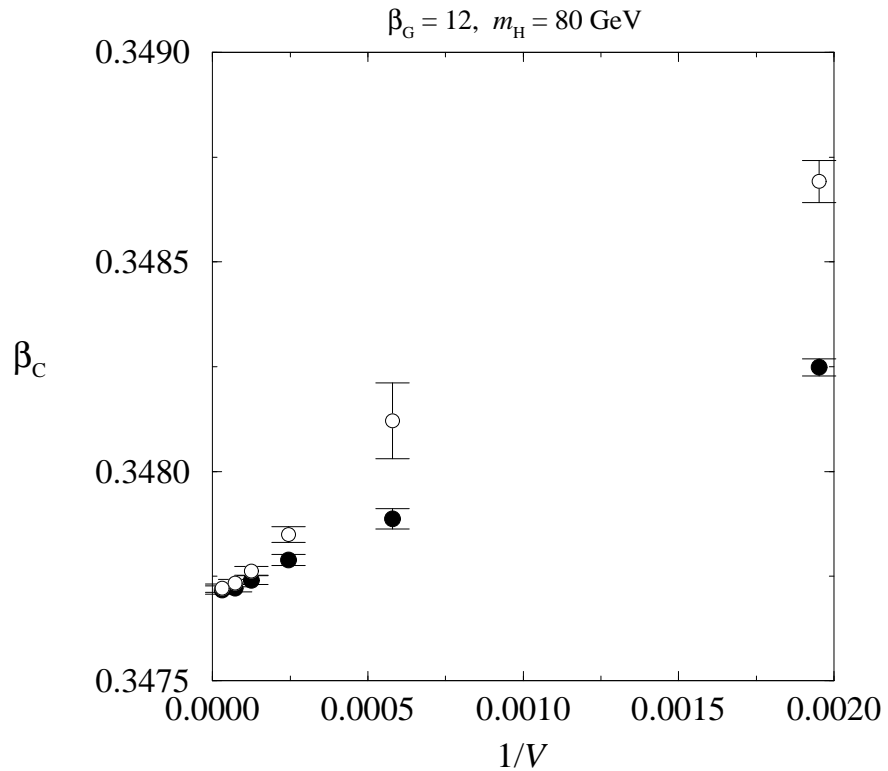


Figure 3: The critical values of  $\beta_H$  for  $m_H = 80 \text{ GeV}$  and  $\beta_G = 12$  for different lattice sizes. The full points correspond to the maximum of  $L$ -susceptibility, and empty points to the maximum of the heat capacity.

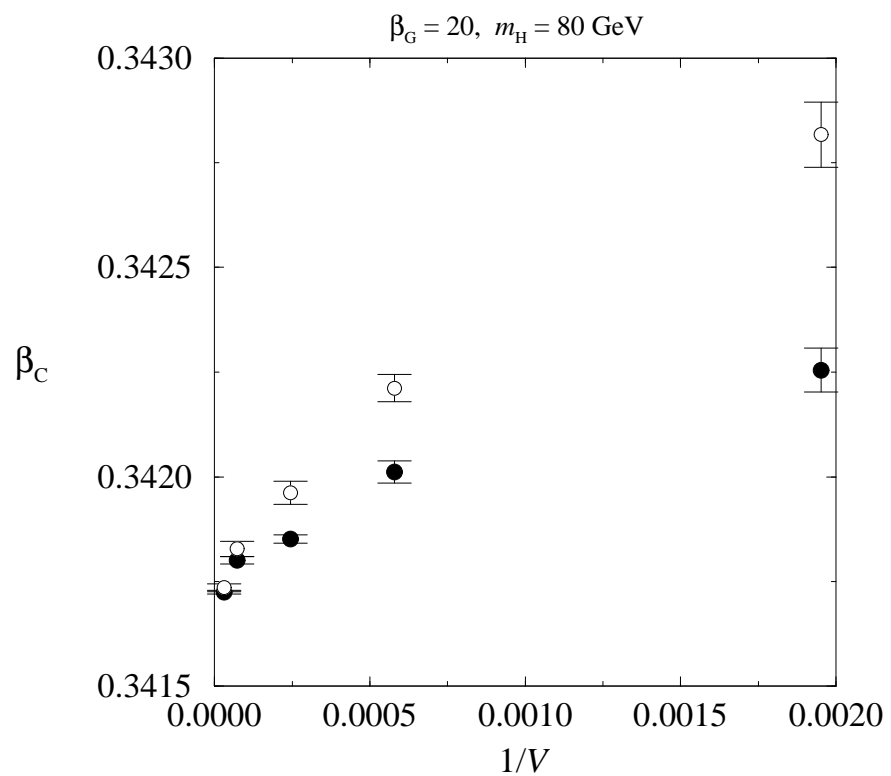


Figure 4: The same as Fig. 3 but for  $\beta_G = 20$

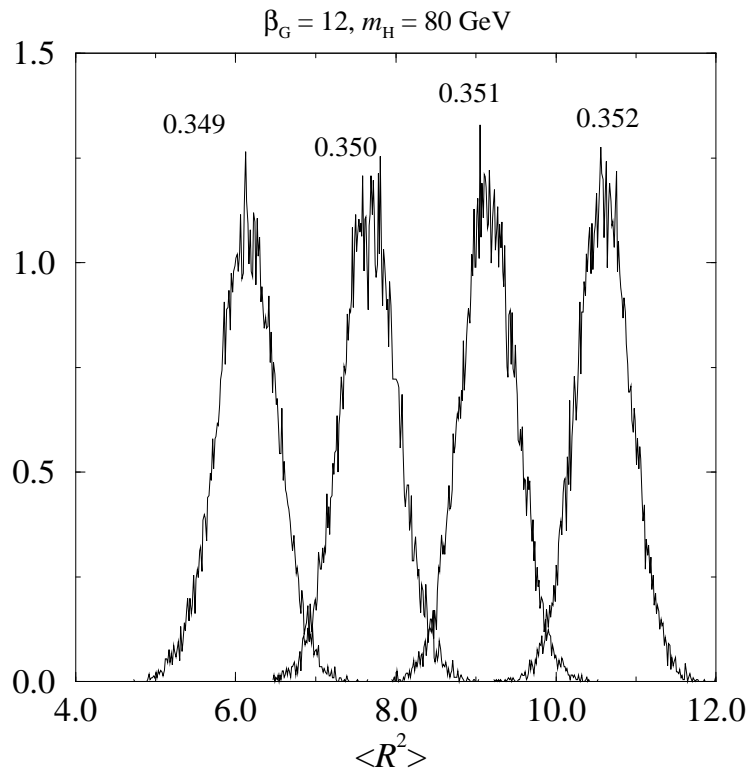


Figure 5: Evolution of the distribution of  $R^2$  in the broken phase with  $\beta_H$  for  $\beta_G = 12$ , with  $m_H = 80 \text{ GeV}$ .

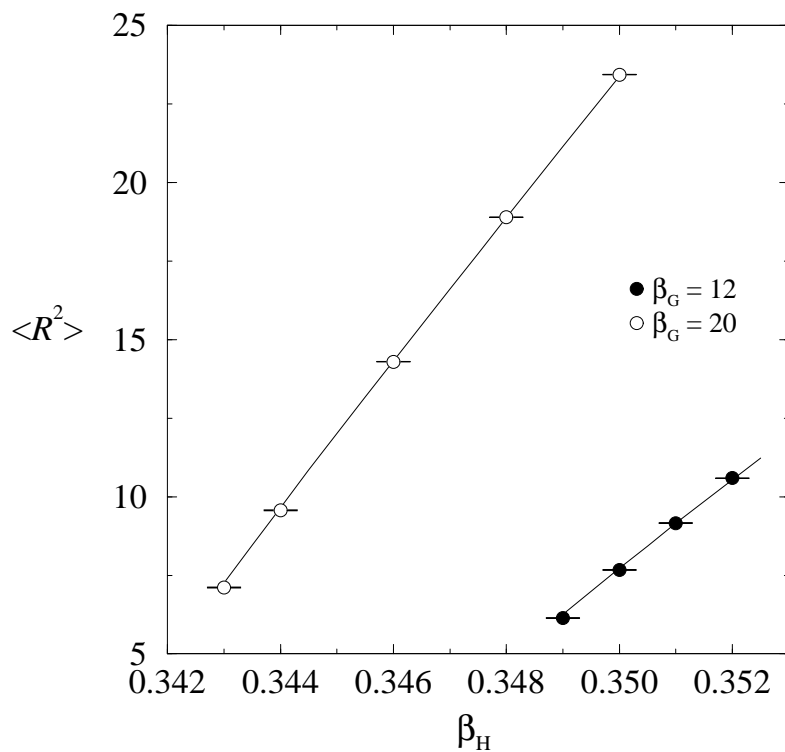


Figure 6:  $\langle R^2 \rangle$  determined on the lattice (points) and by perturbation theory (solid lines). The upper curve corresponds to  $\eta = 0.12$ ,  $\beta_G = 20$  and the lower one to  $\eta = 0.54$ ,  $\beta_G = 12$ .

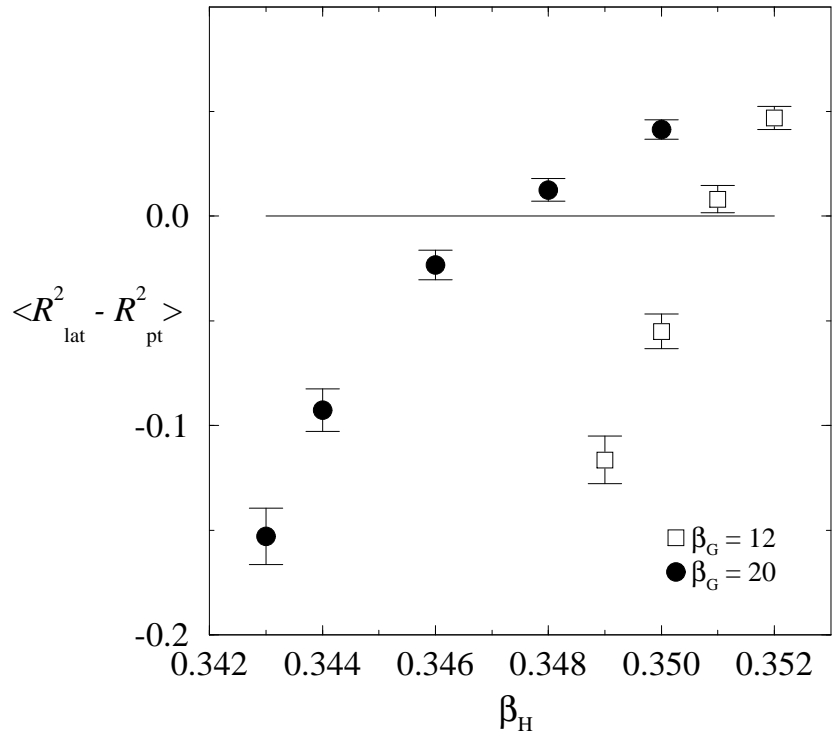


Figure 7: The difference between  $\langle R^2 \rangle$  determined on the lattice and  $\langle R^2 \rangle$  found with the use of perturbation theory for  $\eta = 0.12$ ,  $\beta_G = 20$  and  $\eta = 0.54$ ,  $\beta_G = 12$ .

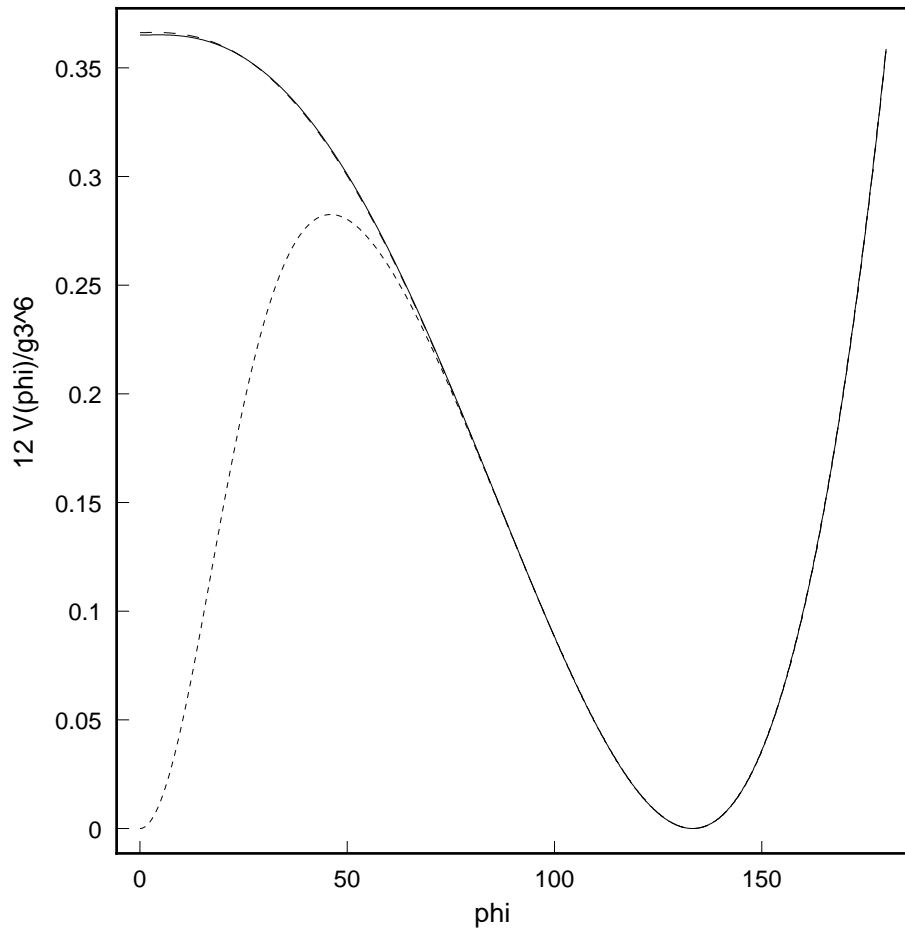


Figure 8: The renormalization group improved effective potential. Solid line - 2-loop order, dashed line - 1-loop order, short-dashed line – possible non-perturbative contribution. The  $x$ -axis is the 4d scalar field in GeV, the  $y$ -axis is the dimensionless effective potential  $12g_3^{-6}V_{eff}(\phi)$ .

This figure "fig1-1.png" is available in "png" format from:

<http://arXiv.org/ps/hep-ph/9405234v1>

This figure "fig1-2.png" is available in "png" format from:

<http://arXiv.org/ps/hep-ph/9405234v1>

This figure "fig1-3.png" is available in "png" format from:

<http://arXiv.org/ps/hep-ph/9405234v1>

This figure "fig1-4.png" is available in "png" format from:

<http://arXiv.org/ps/hep-ph/9405234v1>